FIGURE 8.—Immunohistochemistry for NeuN of the cerebellum from control (left column) and cyclopamine-treated (right column) Ptch1 mice at PND14 (A and B), 21 (C and D), and W12 (E and F). Granular cells of the internal granular layer were strongly positive for NeuN in all animals. In addition, NeuN positive cells were distributed parallel to the Purkinje cell layer in the deeper molecular layer of cyclopamine-treated Ptch1 mice at PND14 (B), 21 (D), and W12 (F). Scale bar: 100 μm.

Note. PND = postnatal day; Ptch1 = patched1; W12 = postnatal week 12.

formation in the cerebellum of Ptch1 mice might result from incomplete inhibitory effects on the MBs. Another possible explanation for these differences is the potency of cyclopamine, which has recently been shown to be only a moderate

inhibitor of hedgehog (Hh) target gene transcription compared to several other more potent synthetic inhibitors of Hh signaling. However, given that cyclopamine was the first Hh signaling inhibitor available, it has been used in many *in vitro* and *in*
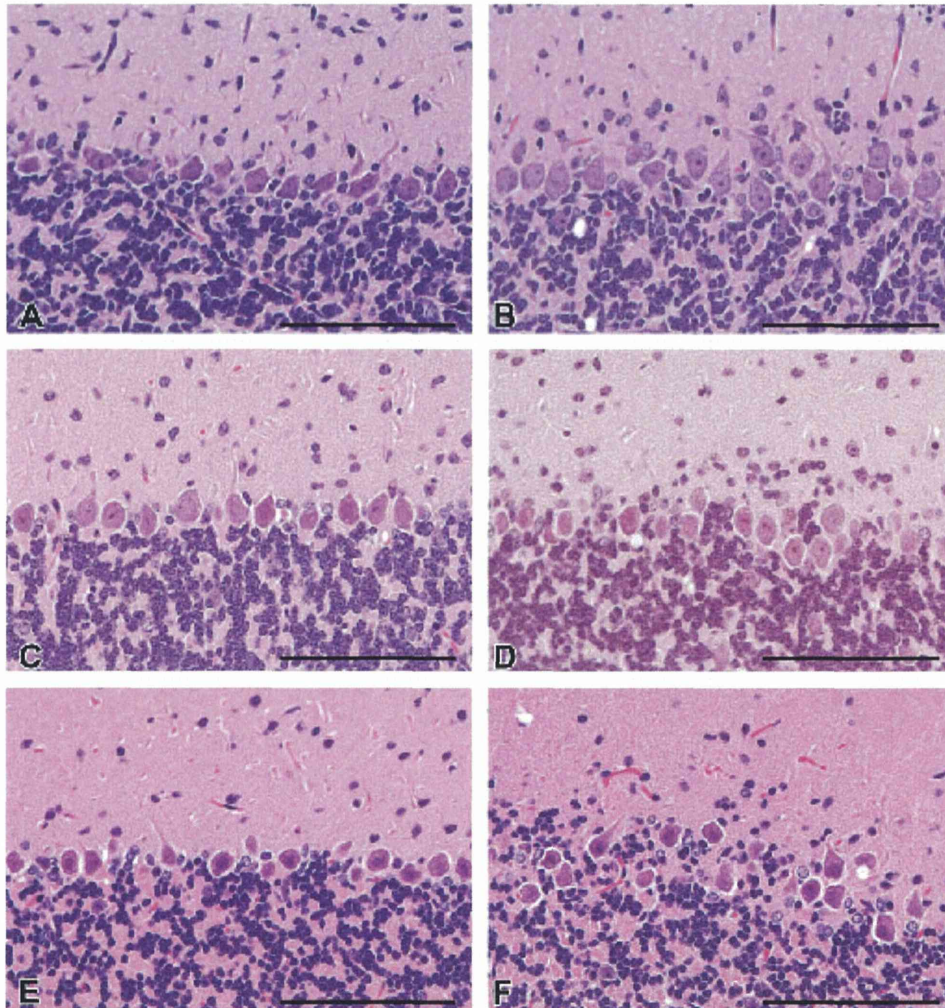
145

FIGURE 9.—Histopathological findings observed in the Purkinje cell layer of the cerebellum from control (left column) and cyclopamine-treated (right column) Ptch1 mice at PND14 (A and B), 21 (C and D), and W12 (E and F) (HE). Misalignment of Purkinje cells was observed in the cyclopamine group at PND14 (B), 21 (D), and W12 (F). Scale bar: 100 µm.
Note. PND = postnatal day; Ptch1 = patched1; W12 = postnatal week 12; HE = hematoxylin and eosin.

vivo studies (Heretsch et al. 2010a and b; Fan et al. 2011; Gupta, Takebe, and Lorusso 2010; Scales and Samvage 2009).

In summary, cyclopamine treatment during cerebellar development has inhibitory effect on proliferation of the EGL and development of MB and preneoplastic lesions in Ptch1 mice, and tendency to inhibit these proliferative lesions is prolonged after treatment. This demonstrates that the Ptch1 mouse is a good model for studying the modifying effects of chemical exposure on MB development during the developmental period.

REFERENCES

Ayrault, O., Zindy, F., Rehg, J., Sherr, C. J., and Roussel, M. F. (2009). Two tumor suppressors, p27Kip1 and patched-1, collaborate to prevent medulloblastoma. *Mol Cancer Res* 7, 33–40.

Bartlett, F., Kortmann, R., and Saran, F. (2013). Medulloblastoma. *Clin Oncol* 25, 36–45.

Behesti, H., and Marino, S. (2009). Cerebellar granule cells: Insights into proliferation, differentiation, and role in medulloblastoma pathogenesis. *Int J Biochem Cell Biol* 41, 435–45.

Berman, D. M., Karhadkar, S. S., Hallahan, A. R., Pritchard, J. I., Eberhart, C. G., Watkins, D. N., Chen, J. K., Cooper, M. K., Taipale, J., Olson, J. M., and Beachy, P. A. (2002). Medulloblastoma growth inhibition by hedgehog pathway blockade. *Science* 297, 1559–61.

Birnbaum, L. S., and Fenton, S. E. (2003). Cancer and developmental exposure to endocrine disruptors. *Environ Health Perspect* 111, 389–94.

Briggs, K. J., Corcoran-Schwartz, I. M., Zhang, W., Harcke, T., Devereux, W. L., Baylin, S. B., Eberhart, C. G., and Watkins, D. N. (2008). Cooperation between the Hic1 and Ptch1 tumor suppressors in medulloblastoma. *Genes Dev* 22, 770–85.

Bunin, G. R., Robison, L. L., Biegel, J. A., Pollack, I. F., and Rorke-Adams, L. B. (2006). Parental heat exposure and risk of childhood brain tumor: A children's oncology group study. *Am J Epidemiol* 164, 222–31.

Coon, V., Laukert, T., Pedone, C. A., Laterra, J., Kim, K. J., and Fults, D. W. (2010). Molecular therapy targeting sonic hedgehog and hepatocyte growth factor signaling in a mouse model of medulloblastoma. *Mol Cancer Ther* 9, 2627–36.

Corcoran, R. B., and Scott, M. P. (2001). A mouse model for medulloblastoma and basal cell nevus syndrome. *J Neurooncol* 53, 307–18.

Dahmane, N., Sanchez, P., Gitton, Y., Palma, V., Sun, T., Beyna, M., Weiner, H., and Ruiz i Altaba, A. (2001). The sonic hedgehog-Gli pathway regulates dorsal brain growth and tumorigenesis. *Development* 128, 5201–12.

Dhall, G. (2009). Medulloblastoma. *J Child Neurol* 24, 1418–30.

Dietrich, M., Block, G., Pogoda, J. M., Buffler, P., Hecht, S., and Preston-Martin, S. (2005). A review: Dietary and endogenously formed N-nitroso compounds and risk of childhood brain tumors. *Cancer Causes Control* 16, 619–35.

Dyer, M. A. (2004). Mouse models of childhood cancer of the nervous system. *J Clin Pathol* 57, 561–76.

Ecke, I., Rosenberger, A., Obenauer, S., Dullin, C., Aberger, F., Kimmina, S., Schweyer, S., and Hahn, H. (2008). Cyclopamine treatment of full-blown Hh/Ptch-associated RMS partially inhibits Hh/Ptch signaling, but not tumor growth. *Mol Carcinog* 47, 361–72.

Ellison, D. W., Dalton, J., Kocak, M., Nicholson, S. L., Fraga, C., Neale, G., Kenney, A. M., Brat, D. J., Perry, A., Yong, W. H., Taylor, R. E., Bailey, S., Clifford, S. C., and Gilbertson, R. J. (2011). Medulloblastoma: Clinicopathological correlates of SHH, WNT, and non-SHH/WNT molecular subgroups. *Acta Neuropathologica* 121, 381–96.

Pan, Q., Gu, D., He, M., Liu, H., Sheng, T., Xie, G., Li, C. X., Zhang, X., Wainwright, B., Garrossian, A., Garrossian, M., Gardner, D., and Xie, J. (2011). Tumor shrinkage by cyclopamine tartrate through inhibiting hedgehog signaling. *Chin J Cancer* 30, 472–81.

Farioli-Vecchioli, S., Tanori, M., Micheli, L., Mancuso, M., Leonardi, L., Saran, A., Ciotti, M. T., Ferretti, E., Gulino, A., Pazzaglia, S., and Tirone, F. (2007). Inhibition of medulloblastoma tumorigenesis by the antiproliferative and pro-differentiative gene PC3. *FASEB J* 21, 2215–25.

Gajjar, A., Stewart, C. F., Ellison, D. W., Kaste, S., Kun, L. E., Packer, R. J., Goldman, S., Chintagumpala, M., Wallace, D., Takebe, N., Boyett, J. M., Gilbertson, R. J., and Curran, T. (2013). Phase I study of vismodegib in children with recurrent or refractory medulloblastoma: A pediatric brain tumor consortium study. *Clin Cancer Res* 19, 6305–12.

Goodrich, L. V., Milenkovic, L., Higgins, K. M., and Scott, M. P. (1997). Altered neural cell fates and medulloblastoma in mouse patched mutants. *Science* 277, 1109–13.

Gupta, S., Takebe, N., and Lorusso, P. (2010). Targeting the Hedgehog pathway in cancer. *Ther Adv Med Oncol* 2, 237–50.

Hahn, H., Wojnowski, L., Miller, G., and Zimmer, A. (1999). The patched signaling pathway in tumorigenesis and development: Lessons from animal models. *J Mol Med* 77, 459–68.

Haldipur, P., Bharti, U., Govindan, S., Sarkar, C., Iyengar, S., Gressens, P., and Mani, S. (2012). Expression of Sonic hedgehog during cell proliferation in the human cerebellum. *Stem Cells Dev* 21, 1059–68.

Hatten, M. E., and Roussel, M. F. (2011). Development and cancer of the cerebellum. *Trends Neurosci* 34, 134–42.

Heretsch, P., Tzagkaroulaki, L., and Giannis, A. (2010a). Cyclopamine and hedgehog signaling: Chemistry, biology, medical perspectives. *Angewandte Chemie* 49, 3418–27.

Heretsch, P., Tzagkaroulaki, L., and Giannis, A. (2010b). Modulators of the hedgehog signaling pathway. *Bioorg Med Chem* 18, 6613–24.

Huse, J. T., and Holland, E. C. (2010). Targeting brain cancer: Advances in the molecular pathology of malignant gliomas and medulloblastoma. *Nat Rev Cancer* 10, 319–31.

Jones, D. T., Jäger, N., Kool, M., Zichner, T., Hutter, B., Sultan, M., Cho, Y. J., Pugh, T. J., Hovestadt, V., Stütz, A. M., Rausch, T., Warnatz, H. J., Ryzhova, M., Bender, S., Sturm, D., Pleier, S., Cin, H., Pfaff, E., Sieber, L., Wittmann, A., Remke, M., Witt, H., Hutter, S., Tzaridis, T., Weischenfeldt, J., Raeder, B., Avci, M., Amstislavskiy, V., Zapatka, M., Weber, U. D., Wang, Q., Lasitschka, B., Bartholomae, C. C., Schmidt, M., von Kalle, C., Ast, V., Lawerenz, C., Eils, J., Kabbe, R., Benes, V., van Sluis, P., Koster, J., Volckmann, R., Shih, D., Betts, M. J., Russell, R. B., Coco, S., Tonini, G. P., Schüller, U., Hans, V., Graf, N., Kim, Y. J., Monoranu, C., Roggendorf, W., Unterberg, A., Herold-Mende, C., Milde, T., Kulozik, A. E., von Deimling, A., Witt, O., Maass, E., Rössler, J., Ebinger, M., Schuhmann, M. U., Frühwald, M. C., Hasselblatt, M., Jabado, N., Rutkowski, S., von Bueren, A. O., Williamson, D., Clifford, S. C., McCabe, M. G., Collins, V. P., Wolf, S., Wiemann, S., Lehrach, H., Brors, B., Scheurlen, W., Felsberg, J., Reifenberger, G., Northcott, P. A., Taylor, M. D., Meyerson, M., Pomeroy, S. L., Yaspo, M. L., Korbel, J. O., Korshunov, A., Eils, R., Pfister, S. M., and Lichter, P. (2012). Dissecting the genomic complexity underlying medulloblastoma. *Nature* 488, 100–5.

Kawauchi, D., Robinson, G., Uziel, T., Gibson, P., Rehg, J., Gao, C., Finkelstein, D., Qu, C., Pounds, S., Ellison, D. W., Gilbertson, R. J., and Roussel, M. F. (2012). A mouse model of the most aggressive subgroup of human medulloblastoma. *Cancer Cell* 21, 168–80.

Kimura, H., Stephen, D., Joyner, A., and Curran, T. (2005). Gli1 is important for medulloblastoma formation in Ptc1 +/− mice. *Oncogene* 24, 4026–36.

Kool, M., Korshunov, A., Remke, M., Jones, D. T., Schlanstein, M., Northcott, P. A., Cho, Y. J., Koster, J., Schouten-van Meeteren, A., van Vuurden, D., Clifford, S. C., Pietsch, T., von Bueren, A. O., Rutkowski, S., McCabe, M., Collins, V. P., Backlund, M. L., Haberler, C., Bourdeaut, F., Delattre, O., Doz, F., Ellison, D. W., Gilbertson, R. J., Pomeroy, S. L., Taylor, M. D., Lichter, P., and Pfister, S. M. (2012). Molecular subgroups of medulloblastoma: An international meta-analysis of transcriptome, genetic aberrations, and clinical data of WNT, SHH, Group 3, and Group 4 medulloblastomas. *Acta Neuropathol* 123, 473–84.

Lee, M. J., Hatton, B. A., Villavicencio, E. H., Khanna, P. C., Friedman, S. D., Ditzler, S., Pullar, B., Robison, K., White, K. F., Tunkey, C., LeBlanc, M., Randolph-Habecker, J., Knoblaugh, S. E., Hansen, S., Richards, A., Wainwright, B. J., McGovern, K., and Olson, J. M. (2012). Hedgehog pathway inhibitor saridegib (IPI-926) increases lifespan in a mouse medulloblastoma model. *PNAS* 109, 7859–64.

Lewis, P. M., Gritli-Linde, A., Smeyne, R., Kottmann, A., and McMahon, A. P. (2004). Sonic hedgehog signaling is required for expansion of granule neuron precursors and patterning of the mouse cerebellum. *Dev Biol* 270, 393–410.

Lipinski, R. J., Hutson, P. R., Hannam, P. W., Nydza, R. J., Washington, I. M., Moore, R. W., Girdaukas, G. G., Peterson, R. E., and Bushman, W. (2008). Dose- and route-dependent teratogenicity, toxicity, and pharmacokinetic profiles of the hedgehog signaling antagonist cyclopamine in the mouse. *Toxicol Sci* 104, 189–97.

Low, J. A., and de Sauvage, F. J. (2010). Clinical experience with Hedgehog pathway inhibitors. *J Clin Oncol* 28, 5321–26.

Matsuo, S., Takahashi, M., Inoue, K., Tamura, K., Irie, K., Kodama, Y., Nishikawa, A., and Yoshida, M. (2013). Thickened area of external granular layer and Ki-67 positive focus are early events of medulloblastoma in Ptch1(+/−) mice. *Exp Toxicol Pathol* 65, 863–79.

McKean-Cowdin, R., Pogoda, J. M., Lijinsky, W., Holly, E. A., Mueller, B. A., and Preston-Martin, S. (2003). Maternal prenatal exposure to nitrosatable drugs and childhood brain tumours. *Int J Epidemiol* 32, 211–17.

Norman, M. A., Holly, E. A., and Preston-Martin, S. (1996). Childhood brain tumors and exposure to tobacco smoke. *Cancer Epidemiol Biomarkers Prev* 5, 85–91.

Northcott, P. A., Korshunov, A., Witt, H., Hielscher, T., Eberhart, C. G., Mack, S., Bouffet, E., Clifford, S. C., Hawkins, C. E., French, P., Rutka, J. T., Pfister, S., and Taylor, M. D. (2011). Medulloblastoma comprises four distinct molecular variants. *J Clin Oncol* 29, 1408–14.

Oliver, T. G., Read, T. A., Kessler, J. D., Mehmeti, A., Wells, J. F., Huynh, T. T., Lin, S. M., and Wechsler-Reya, R. J. (2005). Loss of patched and disruption of granule cell development in a pre-neoplastic stage of medulloblastoma. *Development* 132, 2425–39.

Pazzaglia, S. (2006). Ptc1 heterozygous knockout mice as a model of multiorgan tumorigenesis. *Cancer Lett* 234, 124–34.

Pazzaglia, S., Mancuso, M., Atkinson, M. J., Tanori, M., Rebessi, S., Majo, V. D., Covelli, V., Hahn, H., and Saran, A. (2002). High incidence of medulloblastoma following X-ray-irradiation of newborn Ptc1 heterozygous mice. *Oncogene* 21, 7580–84.

Pazzaglia, S., Pasquali, E., Tanori, M., Mancuso, M., Leonardi, S., di Majo, V., Rebessi, S., and Saran, A. (2009). Physical, heritable and age-related factors as modifiers of radiation cancer risk in patched heterozygous mice. *Int J Radiat Oncol Biol Phys* 73, 1203–10.

Pazzaglia, S., Tanori, M., Mancuso, M., Gessi, M., Pasquali, E., Leonardi, S., Oliva, M. A., Rebessi, S., Di Majo, V., Covelli, V., Giangaspero, F., and Saran, A. (2006). Two-hit model for progression of medulloblastoma preneoplasia in patched heterozygous mice. *Oncogene* 25, 5575–80.

Pogoriler, J., Millen, K., Utset, M., and Du, W. (2006). Loss of cyclin D1 impairs cerebellar development and suppresses medulloblastoma formation. *Development* 133, 3929–37.

Raffel, C. (2004). Medulloblastoma: Molecular genetics and animal models. *Neoplasia* 6, 310–22.

Romer, J. T., Kimura, H., Magdaleno, S., Sasai, K., Fuller, C., Baines, H., Connelly, M., Stewart, C. F., Gould, S., Rubin, L. L., and Curran, T. (2004). Suppression of the Shh pathway using a small molecule inhibitor eliminates medulloblastoma in Ptc1(+/−)p53(−/−) mice. *Cancer Cell* 6, 229–40.

Roussel, M. F., and Hatten, M. E. (2011). Cerebellum development and medulloblastoma. *Curr Top Dev Biol* 94, 235–82.

Sanchez, P., and Ruiz i Altaba, A. (2005). In vivo inhibition of endogenous brain tumors through systemic interference of Hedgehog signaling in mice. *Mech Dev* 122, 223–30.

Scales, S. J., and de Sauvage, F. J. (2009). Mechanisms of Hedgehog pathway activation in cancer and implications for therapy. *Trends Pharmacol Sci* 30, 303–12.

Stecca, B., and Ruiz i Altaba, A. (2002). The therapeutic potential of modulators of the Hedgehog-Gli signaling pathway. *J Biol* 1, 9.

Takahashi, M., Matsuo, S., Inoue, K., Tamura, K., Irie, K., Kodama, Y., and Yoshida, M. (2012). Development of an early induction model of medulloblastoma in Ptch1 heterozygous mice initiated with N-ethyl-N-nitrosourea. *Cancer Sci* 103, 2051–55.

Uziel, T., Zindy, F., Xie, S., Lee, Y., Forget, A., Magdaleno, S., Rehg, J. E., Calabrese, C., Solecki, D., Eberhart, C. G., Sherr, S. E., Plimmer, S., Clifford, S. C., Hatten, M. E., McKinnon, P. J., Gilbertson, R. J., Curran, T., Sherr, C. J., and Roussel, M. F. (2005). The tumor suppressors Ink4c and p53 collaborate independently with patched to suppress medulloblastoma formation. *Genes Dev* 19, 2656–67.

Vaillant, C., and Monard, D. (2009). SHH pathway and cerebellar development. *Cerebellum* 8, 291–301.

Wallace, V. A. (1999). Purkinje-cell-derived Sonic hedgehog regulates granule neuron precursor cell proliferation in the developing mouse cerebellum. *Curr Biol* 9, 445–48.

Wetmore, C., Eberhart, D. E., and Curran, T. (2000). The normal patched allele is expressed in medulloblastomas from mice with heterozygous germ-line mutation of patched. *Cancer Res* 60, 2239–46.

Wetmore, C., Eberhart, D. E., and Curran, T. (2001). Loss of p53 but not ARF accelerates medulloblastoma in mice heterozygous for patched. *Cancer Res* 61, 513–16.

Neonatal Exposure to 17α-Ethinyl Estradiol Affects Kisspeptin Expression and LH-Surge Level in Female Rats

Kento USUDA[1], Kentaro NAGAOKA[1]*, Kaori NOZAWA[1], Haolin ZHANG[1], Kazuyoshi TAYA[1], Midori YOSHIDA[2] and Gen WATANABE[1]

[1] *Laboratory of Veterinary Physiology, Department of Veterinary Medicine, Tokyo University of Agriculture and Technology, 3–5–8 Saiwai-cho, Fuchu-shi, Tokyo 183–8509, Japan*
[2] *Division of Pathology, National Institute of Health Sciences, 1–18–1 Kamiyoga, Setagaya-ku, Tokyo 158–8501, Japan*

ABSTRACT. Contamination of estrogenic compounds disrupts endocrinological and neurological reproductive systems in animals. Neonatal exposure to 17α-ethinyl estradiol (EE) induced an abnormal estrous cycle at postnatal day (PND) 180, but not at PND90. We found that serum level of luteinizing hormone (LH) at the latter half of proestrus in EE-treated rats was lower than in the controls at PND90 when there was no significant difference on estrous cyclicity. Additionally, *kiss1* mRNA levels in the anteroventral periventricular nucleus-preoptic area (AVPV/POA) were lower in EE-treated rats than in the controls. The expression of GnRH precursor (*GNRH1*) mRNA in the AVPV/POA and that of LH beta subunit (*LHb*) mRNA in the pituitary were similar in the control- and EE-treated groups. Our results indicated that neonatal exposure to EE leads to reduced expression of *kiss1* mRNA in AVPV/POA and LH-surge, which is likely related to the delayed reproductive dysfunction seen in adult female rats.
KEY WORDS: 17α-ethinyl estradiol, AVPV/POA, endocrine disruptor, kisspeptin

It has been approximately 20 years since the first World Wildlife Federation (WWF) Wingspread Conference focused on endocrine-disrupting chemicals (EDCs) [11]. EDCs are a broad class of synthetic and natural chemicals, most of which have estrogenic activity [11]. Because these chemicals mimic estrogens that regulate cell fate during embryonic development, exposure to these compounds during the fetal and perinatal periods leads to disruption of endocrinological, neurological and reproductive functions [24].

In rodents, the sexual differentiation of the brain occurs during the late embryonic and early postnatal periods [14]. In males, androgen secreted from the testis passes the Blood-Brain-Barrier (B-B-B) and reaches the brain, where it is converted to estradiol by the action of p450 aromatase enzymes [10]. The estradiol is essential for the normal sexual differentiation of the male brain. In females, the developing ovary secretes estradiol, but most of the circulating estradiol remains bound to α-fetoprotein and cannot pass the B-B-B [21]. Synthetic estrogenic compounds show the ability to escape from binding to α-fetoprotein. Therefore, exposure to synthetic estrogen compounds during the perinatal period may affect the sexual differentiation of the brain in female rodents.

Kisspeptin, a neuropeptide, plays key roles in determining the timing of puberty and regulation of the estrous cycle by stimulating the Hypothalamic-Pituitary-Gonadal axis (HPG axis) [15]. Kisspeptin is expressed in the anteroventral periventricular nucleus (AVPV) and the arcuate nucleus (ARC) [27]. The number of kisspeptin neurons in the AVPV is substantially higher in females than in males, but their numbers in the ARC are not sexually dimorphic [2]. In female mice, the number of the kisspeptin neurons in the AVPV increases after birth and reaches adult levels at the time of puberty [4]. Because kisspeptin neurons express estrogen receptor α (ERα), it is thought that the increase in the number of kisspeptin neurons is regulated by estradiol secreted from the developing ovary. Conditional deletion of ERα from kisspeptin neurons resulted in an arrest in the pubertal maturation and a failure to acquire normal estrous cycle [20].

Kisspeptin acts through binding to the G protein-coupled receptor GPR54 [15]. This receptor is expressed in GnRH neurons, which are primarily located in the preoptic area (POA) and the ARC [15, 17]. Kisspeptin bound to the receptor in POA induces a GnRH-surge followed by an LH-surge [9]. Kisspeptin bound to its receptor in ARC controls the GnRH and LH pulses [17, 18]. Studies have shown that EDCs cause reproductive dysfunction by affecting the population of kisspeptin neurons [7, 26]. However, the effects of EDCs on kisspeptin neurons remain largely uncharacterized.

In this study, we used 17α-ethinyl estradiol (EE) as model EDC. Previous studies found that a one-time administration of EE (20 μg/kg) at postnatal day 1 (PND1) induced abnormal estrous cycle during PND171-190 [22]. To identify the potential changes in kisspeptin neuron following neonatal exposure to EE, we determined the serum levels of reproductive hormones and analyzed the gene expression in AVPV/POA, ARC and pituitary at PND90 before the appearance

*CORRESPONDENCE TO: NAGAOKA, K., Laboratory of Veterinary Physiology, Department of Veterinary Medicine, Tokyo University of Agriculture and Technology, 3–5–8 Saiwai-cho, Fuchu-shi, Tokyo 183–8509, Japan. e-mail: nagaokak@cc.tuat.ac.jp

of the abnormal estrous cycle. Here, we show that neonatal EE exposure leads to a reduction in LH-surge and reduced expression of kisspeptin in AVPV/POA.

MATERIALS AND METHODS

Animals: Adult Wistar-Imamichi rats were maintained in an animal room under standard housing conditions with controlled lighting (lights on from 05 hr 00 to 19 hr 00), temperature ($25 \pm 2°C$) and humidity ($50 \pm 10\%$). Animals were provided with a rat chow diet (MR-Breeder, Nosan Corporation, Yokohama, Japan) and tap water *ad libitum*. All animal experiments were performed in compliance with the guidelines of the Institutional Animal Care and Use Committee of Tokyo University of Agriculture and Technology, Japan.

Experimental design: Figure 1 illustrates the experimental design. The sex ratio of the newborn pups in each litter was adjusted to 6:3 (females: males). Female pups were given one of the following neonatal treatments: 1) sesame oil vehicle alone (control group), 2) EE at 20 μg/kg and 3) EE at 200 μg/kg. These treatments were administered within 24 hr of delivery, on PND0, by subcutaneous (S.C.) injection in the nape of the neck. Once vaginal opening occurred, a daily vaginal smear was collected from each rat and the cytological changes were monitored until PND90 (n=16 for each treatment). At approximately PND90, pups were euthanized at 11 hr 00 on the second diestrous day (D), at 11 hr 00 on the proestrous day (PE11), at 17 hr 00 on the proestrous day (PE17) and at 11 hr 00 on the estrous day (E), and the blood and brains were collected (n=4 for each time point). The blood samples were immediately centrifuged ($1,500 \times g$ for 15 min at $4°C$), and the serum was stored at $-20°C$ until use. The AVPV/POA, the ARC and the pituitary were dissected out from the brain, snap frozen in liquid nitrogen and stored $-80°C$ until further use in RNA extraction. The AVPV/POA and the ARC regions were punched out with the help of a brain punch set (inner diameter of 1.0 mm; Stoeling Corporation, Wheat Lane, Wood Dale, IL, U.S.A. [12]) from the coronal section of the brain following the coordinates provided in the brain atlas (Paxinos and Watson atlas) [16].

Hormone assay: Serum concentrations of LH, follicle stimulating hormone (FSH) and prolactin were measured using a rat radioimmunoassay (RIA) kit (NIH, Bethesda, MD, U.S.A.). The iodinated preparations used were rat LH-I-7, rat FSH-I-7 and PRL-I-6. The antisera used were anti-rat LH-S-10, anti-rat FSH-S-11 and PRL-S-9, respectively. The results were expressed in terms of NIDDK rat LH-RP-3, FSH-RP-2 and PRL-RP3. The intra- and inter-assay coefficients of variations were; 2.7% and 22.08%; 7.1% and 22.75%; and 2.46% and 22.20% for LH, FSH and prolactin, respectively.

The serum concentrations of immunoreactive (ir-) inhibin were measured using the rabbit antiserum against bovine inhibin (TNDH-1) and the ^{125}I-labeled 32-kDa bovine inhibin. Results were expressed as the concentrations of 32-kDa bovine inhibin. The intra- and inter-assay coefficients of variation were 4.77% and 10.30%, respectively.

The serum concentrations of estradiol and testosterone

were measured with the help of a double-antibody RIA system using ^{125}I-labeled radio ligands. Antisera against estradiol (GDN #244) and testosterone (GDN #250) were provided by Dr. G. D. Niswender (Animal Reproduction and Biotechnology, Colorado State University, Fort Collins, CO, U.S.A.). The intra- and inter-assay coefficients of variation were 5.47% and 18.40%, respectively for estradiol and 2.89% and 21.28%, respectively for testosterone.

Quantitative real-time PCR: Total RNA from each sample was extracted using ISOGEN (Nippon Gene, Tokyo, Japan). Complementary DNA (cDNA) was synthesized using PrimeScript reverse transcriptase (TaKaRa Bio, Otsu, Japan) according to the manufacturer's instructions. Oligonucleotide primers were designed using the web-based Primer3 software and are listed in Supplementary Table 1. All polymerase chain reactions were performed using SYBR Premix Ex Taq™ (TaKaRa Bio). The relative expression level of each target mRNA was determined using the $2^{-\Delta\Delta CT}$ method. *GAPDH* or *β-Actin* was used as the endogenous control gene.

Statistical analysis: The data are presented as the mean $\pm$ SEM of values from three independent experiments. The level of significance was analyzed using one-way analysis of variance (ANOVA), followed by multiple range tests (Graph Pad Prism5). Differences with $P<0.05$ were considered statistically significant.

RESULTS

Effect of neonatal EE exposure on reproductive parameters: The changes in body weights are shown in Fig. 2a. The rats in all treatment groups grew normally, and there was no significant difference between the body weights of control and EE-treated groups. The timing of the vaginal opening, which is indicative of puberty, is compared between control and EE-treated groups in Fig. 2b. There was no significant difference between the timing of vaginal opening of the control and EE-treated groups. The time spent in each cycle day at PND90 is shown in Fig. 2c. There was no significant difference in the estrous cycles of all groups at PND90.

Effect of neonatal EE exposure on hormonal changes at PND90: The changes in the serum levels of LH, FSH, inhibin, prolactin, estradiol and testosterone are shown in Fig. 3. LH-surge was observed at PE17, and the peak levels were reduced in the EE-treated groups compared to control group. In 200 μg/kg EE-treated group, increases of FSH at diestrous and testosterone at PE11 were observed (Fig. 3b and 3e). There were no significant differences in the levels of other hormones between control and EE-treated groups.

Effect of neonatal EE exposure on hypothalamic gene expression at PND90: To examine the potential hypothalamic changes in EE-treated animals, the kisspeptin (*kiss1*), *GPR54*, *ERα* and *GNRH1* mRNA levels in the AVPV/POA and the ARC regions were quantified by quantitative real-time PCR. EE treatment reduced the levels of *kiss1* mRNA in the AVPV/POA at PE17 (Fig. 4a). In 200 μg/kg EE-treated group, decrease of GNRH1 mRNA expression at diestrous was observed (Fig. 4d). There were no significant differences in the mRNA levels of *GPR54* and *ERα* (Fig. 4b and
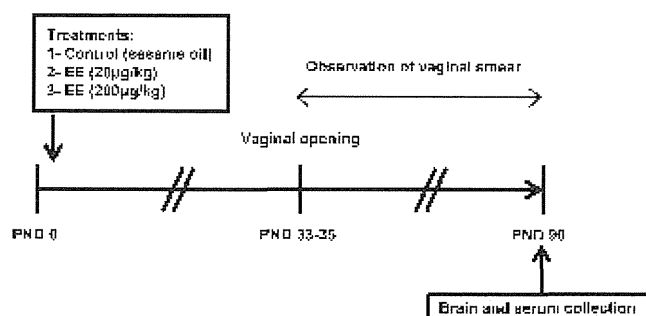
Fig. 1. Schematic representation of experimental protocol. PND, postnatal day.
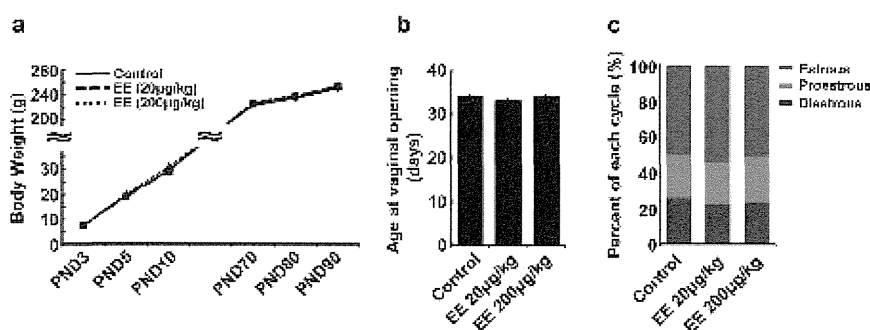

Fig. 2. Effect of neonatal EE exposure on body weight and reproductive parameters. (a) Body weight from PND3 to PND10 and from PND70 to PND90. PND, postnatal day. (b) Age at vaginal opening. (c) Percent of time spent in each cycle day during PND75-90. Rats were neonatally treated with sesame oil and with 2 concentrations of EE (20 μg/kg and 200 μg/kg). Estrous stage was determined by vaginal cytology. Data are presented as the mean ± SEM.

4c). Compared to controls, the expression of *kiss1* mRNA in the ARC of 200 μg/kg EE-treated group was lower at PE17 (Fig. 5a). However, there were no significant differences in the mRNA levels of *GPR54*, *ERα* and *GNRH1* between the ARCs of control and EE-treated groups (Fig. 5b, 5c and 5d).

Effect of neonatal EE exposure on pituitary gene expression at PND90: The mRNA levels of *LHb*, FSH beta subunit (*FSHb*), prolactin (*PRL*) and GnRH receptor (*GNRHR*) were determined by quantitative real-time PCR (Fig. 6). There were no significant differences in the mRNA expression levels of other genes between the control and the treatment groups.

DISCUSSION

It has been reported that the perinatal exposure to EDCs affects the HPG axis and the brain development related to sexual differentiation. Here, we report EE-induced changes

that are potentially related to the delayed reproductive dysfunction. Neonatal EE exposure caused a reduction in the LH-surge level at PND90 when the animals showed a normal estrous cycle. In contrast, these animals showed abnormal estrous cycle at PND180. Reduced *kiss1* mRNA expression was also observed in the AVPV/POA of EE-treated animals. It has been reported that in males, no LH-surge occurred and the expression level of kisspeptin in the AVPV/POA was lower in males than females [1, 2]. Neonatal exposure of neonatal females to EE might induce the masculinization of the AVPV/POA region during the sexual differentiation of the brain, which is likely the reason for the reduced kisspeptin gene expression and the low LH-surge at PND90.

In this study, we administered EE (20 and 200 μg/kg) to pups subcutaneously at PND0. The EE has been widely used for oral contraception in women, and the pills contain 50 μg EE, corresponding to 1.0 μg/kg/day. The doses selected in this study were approximately 20-200 times higher than
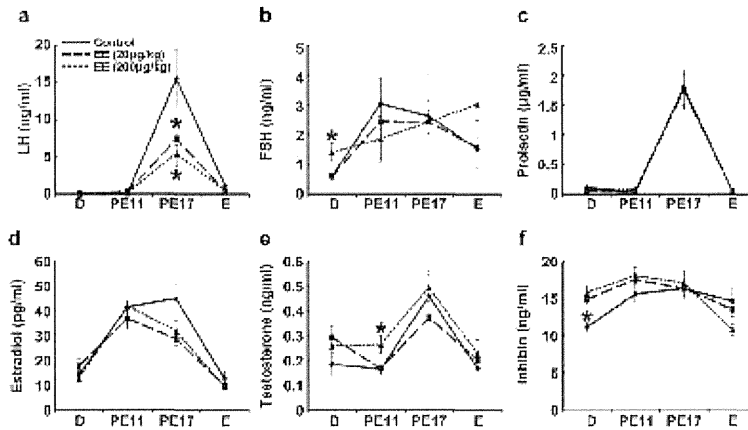
Fig. 3.   Changes in serum level of LH (a), FSH (b), prolactin (c), estradiol-17β (d), testosterone (e) and inhibin (f) in neonatal EE treated rats. Bloods were collected at PND90 from animals treated with sesame oil and with 2 concentrations of EE (20 μg/kg and 200 μg/kg). Hormone level was measured by RIA. Each point represents mean ± SEM. Asterisk indicates a significant difference compared to the control (P<0.05). D, Diestrous PE11, Proestrous at 11 hr 00 PE17, Proestrous at 17 hr 00 E, Estrous.
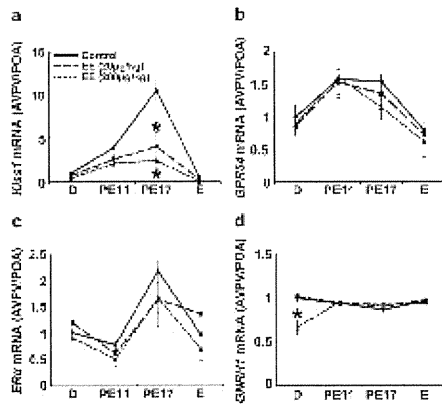

Fig. 4.   Changes in kiss1 (a), GPR54 (b), ERα (c) and GNRH1 (d) mRNA expression in AVPV/POA. Samples were collected at PND90 from animals treated with sesame oil and with two concentrations of EE (20 μg/kg and 200 μg/kg). mRNA expression level was analyzed by real-time PCR. Each point represents mean ± SEM. Asterisk indicates a significant difference compared to the control (P<0.05). D, Diestrous PE11, Proestrous at 11 hr 00 PE17, Proestrous at 17 hr 00 E, Estrous.

Fig. 5.   Changes in kiss1 (a), GPR54 (b), ERα (c) and GNRH1 (d) mRNA expression in ARC. Samples were collected at PND90 from animals treated with sesame oil and with 2 concentrations of EE (20 μg/kg and 200 μg/kg). mRNA expression level was analyzed by real-time PCR. Each point represents mean ± SEM. Asterisk indicates a significant difference compared to the control (P<0.05). D, Diestrous PE11, Proestrous at 11 hr 00 PE17, Proestrous at 17 hr 00 E, Estrous.
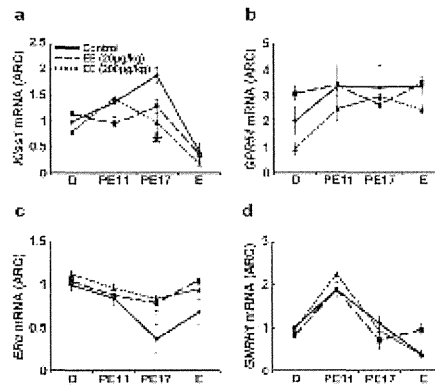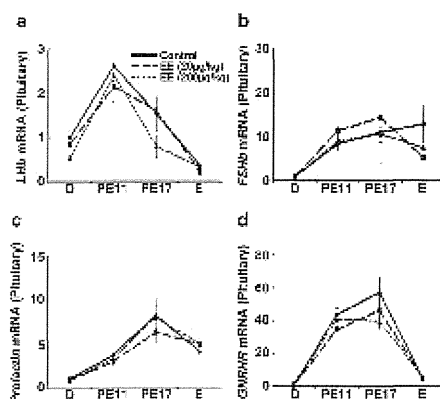
Fig. 6. Changes in *LHb* (a), *FSHb* (b), prolactin (c) and *GNRHR* (d) mRNA expression in pituitary. Samples were collected at PND90 from animals treated with sesame oil and with 2 concentrations of EE (20 μg/kg and 200 μg/kg). mRNA expression level was analyzed by real-time PCR. Each point represents mean ± SEM. Asterisk indicates a significant difference compared to the control (*P*<0.05). D, Diestrous PE11, Proestrous at 11 hr 00 PE17, Proestrous at 17 hr 00 E, Estrous.

exposure of women. In a previous study, EE (5–50 μg/kg/day) was administered to dams by oral gavage from gestational day (GD) 7 to PND22 [18]. The authors reported that there were no changes in the *kiss1* mRNA expression in the AVPV/POA of pups at PND50 [18]. However, the quantity of EE that reached the pup's circulation is not known. The lower chronic exposure was not sufficient to induce changes in *kiss1* gene expression. It is likely that the metabolism of EE in the mother's body, placenta and mammary gland might prevent EE from entering the pup's circulation. Therefore, the timing and method of administration should be prescribed for a comprehensive assessment of the effects of EE.

Estrogen regulates *kiss1* mRNA expression in kisspeptin neurons [15]. Two distinct subtypes of ER, ERα and ERβ, are known [21]. *ERα* is predominantly expressed in the uterus, mammary gland, testis, pituitary, liver and kidney, whereas *ERβ* is primarily expressed in the ovary and prostate [6]. Kisspeptin neurons highly express high levels of ERα, which is higher in females than in males [3, 16, 25]. Estrogen fails to stimulate *kiss1* mRNA expression in kisspeptin neurons of the ovariectomized ERα-knockout mice [28]. Thus, ERα mediates estrogen-induced *kiss1* gene expression [5]. Our results showed that the expression level of ERα in the AVPV/POA and the ARC of the control- and EE-treated groups was similar. Additionally, serum level of estrogen was unaffected by EE treatment. Taken together, the reduced expression of *kiss1* mRNA in the AVPV/POA of EE-treated animals may have been due to a functional impairment of signaling downstream of ER.

The serum LH-surge levels decreased along with the reduction in the level of *kiss1* mRNA. Generally, kisspeptin controls LH levels through activating GnRH neuron. GnRH-surge released from the AVPV/POA stimulates pituitary gonadotroph to induce LH-surge without stimulating the transcription. GnRH-pulse generated from the ARC controls basal LH and FSH expression. The AVPV/POA and ARC contained GnRH neurons and we investigated the expression levels of *GNRH1* and *GPR54* mRNA, however, there were no significant differences in both regions. Furthermore, the expression of *LHb* and *GNRHR* mRNA remained unchanged in the pituitary. In 200 μg/kg EE-treated group, the serum FSH showed irregular changes during the estrus cycle, but the expression of *FSHb* mRNA did not change in the pituitary. It was reported that kisspeptin also elicits FSH secretion and intracerebroventricular administration of kisspeptin peptide stimulated FSH secretion in prepubertal and adult rats [23, 27]. These observations provided the possibility that the decrease in LH-surge and irregular FSH might be linked to the weaken GnRH neuron activity and/or reduced GnRH secretion via down-expressed kisspeptin in the AVPV/POA and ARC of EE-treated animals.

In conclusion, we showed that neonatal exposure to EE leads to reduced kisspeptin expression in the AVPV/POA and reduced LH-surge, which is likely involved in the delayed reproductive dysfunction in the adult animals. Previous studies have found that when compared to young rats exhibiting normal estrous cycle, middle-aged rats with persistent estrous had low LH-surge and lower percentage of *kiss1* mRNA-positive neurons with c-fos immunoreactivity in the AVPV [8, 13, 19, 29]. Since there are some similarities on reproductive phenotypes between neonatal EE exposure animals and middle-aged animals, neonatal EE administration may be useful for generating animal models to investigate the physiological and molecular mechanisms of reproductive aging. Further studies are needed to identify the mechanisms responsible for the suppression of kisspeptin expression following exposure to EE.

REFERENCES

1. Bai, Y., Chang, F., Zhou, R., Jin, P. P., Matsumoto, H., Sokabe, M. and Chen, L. 2011. Increase of anteroventral periventricular kisspeptin neurons and generation of E2-induced LH-surge systems in male rats exposed perinatally to environmental dose of bisphenol-A. *Endocrinology* 152: 1562–1571. [Medline] [CrossRef]
2. Bateman, H. L. and Patisaul, H. B. 2008. Disrupted female reproductive physiology following neonatal exposure to phytoestrogens or estrogen specific ligands is associated with decreased GnRH activation and kisspeptin fiber density in the hypothalamus. *Neurotoxicology* 29: 988–997. [Medline] [CrossRef]
3. Cao, J. and Patisaul, H. B. 2011. Sexually dimorphic expression of hypothalamic estrogen receptors α and β and kiss1 in neonatal

male and female rats. *J. Comp. Neurol.* 519: 2954–2977. [Medline] [CrossRef]

4. Clarkson, J. and Herbison, A. E. 2006. Postnatal development of kisspeptin neurons in mouse hypothalamus: Sexual dimorphism and projections to gonadotropin-releasing hormone neurons. *Endocrinology* 147: 5817–5825. [Medline] [CrossRef]

5. Clarkson, J., Boon, W. C., Simpson, E. R. and Herbison, A. E. 2009. Postnatal development of an estradiol-kisspeptin positive feedback mechanism implicated in puberty onset. *Endocrinology* 150: 3214–3220. [Medline] [CrossRef]

6. Couse, J. F. and Korach, K. S. 1999. Estrogen receptor null mice: what have we learned and where will they lead us? *Endocr. Rev.* 20: 358–417. [Medline] [CrossRef]

7. Dickerson, S. M., Cunningham, S. L., Patisaul, H. B. P., Woller, M. J. and Gore, A. C. 2011. Endocrine disruption of brain sexual differentiation by developmental PCB exposure. *Endocrinology* 152: 581–594. [Medline] [CrossRef]

8. Downs, J. L. and Wise, P. M. 2009. The role of the brain in female reproductive aging. *Mol. Cell. Endocrinol.* 299: 32–38. [Medline] [CrossRef]

9. Garcia-Galiano, D., Pinilla, L. and Tena-Sempere, M. 2012. Sex steroids and the control of the kiss1 system: Developmental roles and major regulatory actions. *J. Neuroendocrinol.* 24: 22–33. [Medline] [CrossRef]

10. Gore, A. C. 2008. Developmental programming and endocrine disruptor effects on reproductive neuroendocrine systems. *Front. Neuroendocrinol.* 29: 358–374. [Medline] [CrossRef]

11. Hotchkiss, A. K., Rider, C. V., Blystone, C. R., Wilson, V. S., Hartig, P. C., Ankley, G. T., Foster, P. M., Gray, C. L. and Gray, L. E. 2008. Fifteen years after "wingspread"–environmental endocrine disruptors and human and wildlife health: Where we are today and where we need to go. *Toxicol. Sci.* 105: 235–259. [Medline] [CrossRef]

12. Horii, Y., Dalpatadu, S. L., Soga, T., Ohta, R., Watanabe, G., Taya, K. and Parhar, I. S. 2013. Estrogenic regulation of kiss1 mRNA variants in Hatano rats. *Gen. Comp. Endocrinol.* 181: 246–253. [Medline] [CrossRef]

13. Ishii M. N., Matsumoto, K., Matsui H., Seki, N., Matsumoto, H., Ishikawa, K., Hatani, F., Watanabe, G. and Taya, K. 2013. Reduced responsiveness of kisspeptin neurons to estrogenic positive feedback associated with age-related disappearance of LH surge in middle- age female rats. *Gen. Comp. Endocrinol.* 193: 121–129. [Medline] [CrossRef]

14. Juraska, J. M., Sisk, C. L. and Doncarlos, L. L. 2013. Sexual differentiation of the adolescent rodent brain: Hormonal influences and developmental mechanisms. *Horm. Behav.* 64: 203–210. [Medline] [CrossRef]

15. Kauffman, A. S., Gottsch, M. L., Roa, Byquist, A. C., Crown, A. and Clifton, D. K. 2007. Sexual differentiation of kiss1 gene expression in the brain of the rat. *Endocrinology* 148: 1774–1783. [Medline] [CrossRef]

16. Li, X. F., Kinsey-Jones, J. S., Cheng, Y., Knox, A. M. I., Lin, Y. and Petrou, N. A. 2009. Kisspeptin signalling in the hypothalamic arcuate nucleus regulates GnRH pulse generator frequency in the rat. *PLoS ONE* 4. [Medline] [CrossRef]

17. Maeda, K., Ohkura, S., Uenoyama, Y., Wakabayashi, Y., Oka, Y., Tsukamura, H. and Okamura, H. 2010. Neurobiological mechanisms underlying GnRH pulse generation by the hypothalamus.

Brain Res. 1364: 103–115. [Medline] [CrossRef]

18. Matt, D. W., Glison, M. P., Sales, T. E., Krieg, R. J., Kerbeshian, M. C., Veldhuis, D. and Evans, W. S. 1998. Characterization of attenuated proestrous luteinizing hormone surge in middle-aged rats by deconvolution analysis. *Biol. Reprod.* 59: 1477–1482. [Medline] [CrossRef]

19. Mayer, C., Martinez, M. A., Dubois, S. L., Wolfe, A., Radovick, S., Boehm, U. and Levine, J. E. 2010. Timing and completion of puberty in female mice depend on estrogen receptor α-signaling in kisspeptin neurons. *Proc. Natl. Acad. Sci. U.S.A.* 107: 22693–22698. [Medline] [CrossRef]

20. De Mees, C., Laes, J. F., Bakker, J., Smitz, J., Hennuy, B. and Vooren, P. V. 2006. Alpha-fetoprotein controls female fertility and prenatal development of the gonadotropin-releasing hormone pathway through an antiestrogenic action. *Mol. Cell. Biol.* 26: 2012–2018. [Medline] [CrossRef]

21. Mueller, S. O. and Korach, K. S. 2001. Estrogen receptors and endocrine diseases: lessons from estrogen receptor knockout mice. *Curr. Opin. Pharmacol.* 1: 613–619. [Medline] [CrossRef]

22. Nozawa, K., Nagaoka, K., Zhang, H., Usuda, K., Okazaki, S., Taya, K. and Watanabe, G. 2014. Neonatal exposure to 17α-ethynyl estradiol affect ovarian gene expression and causes reproductive dysfunction in female rats. *Reprod. Toxicol.* (in press). [CrossRef]

23. Navarro, V. M., Castellano, J. M., Fernandez-Fernandez, R., Tovar, S., Roa, J., Mayan, A., Barreiro, M. L., Casanueva, F. F., Aguilar, E., Dieguez, C., Pinilla, L. and Tena-Sempere, M. 2005. Effects of KISS-1 peptide, the natural ligand of GPR54, on follicle-stimulating hormone secretion in the rat. *Endocrinology* 146: 1689–1697. [Medline] [CrossRef]

24. Ohta, R., Ohmukai, H., Marumo, H., Shindo, T., Nagata, T. and Ono, H. 2012. Delayed reproductive dysfunction in female rats induced by early life exposure to low- dose diethylstilbestrol. *Reprod. Toxicol.* 34: 323–330. [Medline] [CrossRef]

25. Okamura, H., Yamamura, T. and Wakabayashi, Y. 2013. Kisspeptin as a master player in the central control of reproduction in mammals: An overview of kisspeptin research in domestic animals. *Anim. Sci. J.* 84: 369–381. [Medline] [CrossRef]

26. Overgaard, A., Holst, K., Mandrup, K. R., Boberg, J., Christiansen, S., Jacobsen, P. R., Hass, U. and Mikkelsen, J. D. 2013. The effect of perinatal exposure to ethinyl oestradiol or a mixture of endocrine disrupting pesticides on kisspeptin neurons in the rat hypothalamus. *Neurotoxicology* 37: 154–162. [Medline] [CrossRef]

27. Pinilla, L., Aguilar, E., Dieguez, C., Millar, R. P. and Sepere, T. 2012. Kisspeptins and reproduction: physiological roles and regulatory mechanisms. *Physiol. Rev.* 92: 1235–1316. [Medline] [CrossRef]

28. Smith, J. T., Cunningham, M. J., Rissman, E. F., Clifton, D. K. and Steiner, R. A. 2005. Regulation of kiss1 gene expression in the brain of the female mouse. *Endocrinology* 146: 3686–3692. [Medline] [CrossRef]

29. Zhang, J., Yang, L., Lin, N., Pan, X., Zhu, Y. and Chen, X. 2014. Aging- related changes in the RP3V kisspeptin neurons predate the reduced activation of GnRH neurons during the early reproductive decline in female mice. *Neurobiol. Aging* 35: 655–668. [Medline] [CrossRef]

Contents lists available at ScienceDirect

Reproductive Toxicology

Prior attenuation of KiSS1/GPR54 signaling in the anteroventral periventricular nucleus is a trigger for the delayed effect induced by neonatal exposure to 17alpha-ethynylestradiol in female rats

Ryohei Ichimura [a,b,c], Miwa Takahashi [a], Tomomi Morikawa [a], Kaoru Inoue [a], Jun Maeda [a,d], Kento Usuda [b], Makoto Yokosuka [e], Gen Watanabe [b], Midori Yoshida [a,*]

[a] Division of Pathology, National Institute of Health Science, 1-18-1 Kamiyoga, Setagaya, Tokyo 158-8501, Japan
[b] Laboratory of Veterinary Physiology, Department of Veterinary Medicine, Tokyo University of Agriculture and Technology, 3-5-8 Saiwai-cho, Fuchu, Tokyo 183-8509, Japan
[c] Development Research, Pharmaceutical Research Center, Mochida Pharmaceutical Co., Ltd., 722 Jimba-aza-Uenohara, Gotemba, Shizuoka 412-8524, Japan
[d] Laboratory of Molecular Pharmacology, Biosignal Research Center, Kobe University, 1-1 Rokkodai-cho, Nada, Kobe 657-8501, Japan
[e] Behavioral Neuroscience Laboratory, Graduate School of Veterinary Medicine, Nippon Veterinary and Life Science University, 1-7-1 Kyonan-cho, Musashino, Tokyo 180-8602, Japan

ABSTRACT

Neonatal exposure to 17alpha-ethynylestradiol (EE) causes delayed effect, a late-occurring irreversible damage to reproductive functions characterized by the early onset of age-matched abnormal estrous cycling. To clarify the involvement of a hypothalamic key cycling regulator KiSS1/GPR54 in the delayed effect, we investigated artificially induced LH surges and KiSS1 mRNA expression in the anteroventral periventricular nucleus (AVPV) of cycling young adult rats neonatally exposed to EE, and compared these parameters to those in about 5 months old middle-aged rats. KiSS1 mRNA expression, the number of KiSS1-positive cells and KiSS1/ERα co-expressing cells in the AVPV decreased in both EE-exposed and middle-aged rats. The peak area and levels of LH surge dose-dependently decreased in EE-exposed rats, and reduction was more evident in middle-aged rats. These results indicate that the prior attenuation of KiSS1 and consequent depression of LH surges plays a key role in the onset of abnormal estrous cycling in the delayed effect.

© 2015 Elsevier Inc. All rights reserved.

1. Introduction

Exposure to the endocrine disrupting chemicals (EDCs) contained in man-made chemicals such as pesticides, plasticizers and drug medicines, has been a major concern for human health because EDCs possess exogenous estrogenic activity and interfere with normal physiological systems and hormone balance, potentially induce various adverse effects on hormones regulating reproductive functions in human being and wildlife [1,2]. It is widely known that prenatal and neonatal exposure to estrogens can cause irreversible, complex damage to the hypothalamus–pituitary–gonadal (HPG) axis and disrupt the programming of endocrine signaling pathways during early developmental stages in mammals [3,4]. For example, neonatal exposure to large amounts of various estrogenic compounds during critical periods of development have a serious influence on the sex differentiation of the brain, causing various irreversible abnormalities, such as masculinized sexual behavior, lower gonadotropin levels in puberty, malformation of the reproductive tract, and cessation of cyclic ovulation [5–7]. These effects are known as "defeminization" or "masculinization" of female sexual behavior and reproductive functions and these abnormalities are usually manifested during the pre- or peri-pubertal periods.

On the other hand, shorter and lower-dose neonatal exposure to estrogenic compounds like EDCs also causes multiple adverse

effects on female reproductive functions, but the timing of appearance and type of effects are reported to be different from that observed in "musculinization". For instance, neonatal or perinatal exposure to chemicals such as p-t-octylphenol, methoxychlor or a synthetic estrogen, diethylstilbestrol, are reported to induce early onset of abnormal estrous cycle, advanced reproductive senescence and increased uterine carcinogenic risk in young adult or aging rat [8–10]. In these animals, reproductive tracts are known to normally develop and normal estrous cycles were also observed after the vaginal opening; however, the early onset of age-matched abnormal estrous cycle become apparent in young adult age, and increased carcinogenic risk due to the chronic increase of estrogen/progesterone ratio were observed later in life [9–11]. These late-occurring adverse effects are recognized as "delayed effects" or "delayed reproductive dysfunction" in the previous reports [10–13], and could be defined as various reproductive dysfunctions having the following features; 1) be induced by the perinatal exposure to relatively low-dose of estrogenic compounds, and 2) manifest after the peripubertal period in association with the early cessation of estrous cycle. Disruption of the hypothalamic cycle regulating center in early developmental stages has been considered as one of the major mechanism of the delayed effect; however, the precise mechanism underlying the delayed effect remains unknown [10,11]. Moreover, the potential of compounds like EDCs to induce the delayed effect might be overlooked in short-term bioassay and existing developmental toxicity studies, because the delayed effect usually becomes apparent only after the general observation period of most authorized reproductive toxicity studies. Therefore, investigation and elucidation of the mechanism and exploration of the early indicator of delayed effect are toxicologically important for the risk assessment of these estrogenic compounds.

Kisspeptin, the endogenous ligand of the G-protein-coupled receptor GPR54 (KiSS1R) previously called metastin [14,15], is now recognized as playing critical roles in various female reproductive functions and in the regulation of estrous cycling [16,17]. Kisspeptin is a neuropeptide encoded by the KiSS1 gene and regulates GnRH/LH secretion in the HPG axis [17,18]. In the rat brain, the population of Kisspeptin neurons is located mainly in two specific areas of the hypothalamus: the anteroventral periventricular nucleus (AVPV) and the arcuate nucleus (ARC). Interestingly, each area is considered to play a site-specific role: the AVPV triggers the surge in secretion of GnRH, leading to ovulation in the normal estrous cycle, and the ARC induces GnRH pulsatile secretion, which is responsible for follicular development [17–19]. A number of recent studies focused on kisspeptin-GPR54 have revealed that this neurotransmission pathway is the target of estrogen feedback systems in the HPG axis, i.e., activation of kisspeptin neurons is regulated by ovarian estrogens and receives positive feedback in the AVPV or negative feedback in the ARC via estrogen receptors expressed on kisspeptin neurons themselves [20–22]. Regarding cyclic ovulation control, activated kisspeptin neurons secrete kisspeptin in the AVPV and consequently activate GnRH secretion, which induces the transient secretion of large amounts of LH from the pituitary (LH surge) and leads to cyclic ovulation in the normal estrous cycle [23–25]. Since these reproductive functions are unique to female animals, the number of kisspeptin neurons in the AVPV is known to be markedly sexually dimorphic [26,27].

Previously, we reported that neonatal exposure to 17alpha-ethynylestradiol (EE) causes an age- and dose-dependent delayed effect, characterized by an increased incidence of early onset of abnormal estrous cycling from 10 to 22 weeks of age [11]. This abnormal estrous cycling is mainly persistent estrus, which is similar to the age-related persistent estrus observed in the middle-aged female rat. Since no abnormalities in ovarian follicles were detected in these animals, disruption of the HPG axis, especially of the luteinizing hormone (LH) surge and hypothalamic KiSS1/GPR54

signaling are predicted. In fact, there are a few reports that show a significant decrease in KiSS1 mRNA expression and kisspeptin-immunoreactivity in the hypothalamic kisspeptin neurons in middle-aged rats [28,29] and in animals neonatally exposed to various estrogenic compounds [30–32]. However, the selected dose in these reports are extremely high, and sufficient to cause the "masculinization" of the female brain; therefore, the contribution of kisspeptin to the occurrence of delayed effects induced by low-dose neonatal exposure to estrogenic compounds remains unclear.

In the present study, we investigate the artificial LH surge and KiSS1 mRNA expression in the anterior/posterior hypothalamus of neonatal EE-exposed and middle-aged ovariectomy (OVX) rats to elucidate the functional changes of kisspeptin neuron in the delayed effect and in middle-aged rats, and to explore the potential of changes in kisspeptin neurons as early toxicological indicators of the delayed effect.

2. Materials and methods

2.1. Animals

Pregnant Crj:Donryu rats maintained in house were prepared for Experiment 1 (n = 40) and Experiment 2 (n = 28). This strain is known to show regular 4-days cycle after puberty [8]. The rats were housed individually in polycarbonate cages with wood chip bedding and maintained in an air-conditioned animal room (temperature, 24 ± 1 °C; relative humidity, 55 ± 5%; 12-h light/dark cycle: light on, 5:00–17:00; light off, 17:00–5:00) with a basal diet (CRF-1; Oriental Yeast Co., Tokyo, Japan) and tap water available ad libitum. CRF-1 is a standard diet that includes soy protein and is known to contain a relatively low level of estrogens. The animal protocol was reviewed and approved by the Animal Care and Use Committee of the National Institute of Health Sciences (Japan).

2.2. Chemicals

EE (CAS No. 57-63-6) with purity >98% was purchased from Sigma (St. Louis, MO, USA). EE was stirred in a small amount of sesame oil overnight, then used after dilution. EE was selected because of its rapid excretion and lower binding affinity for α-fetoprotein in neonatal blood, so as to limit the exposure time to the neonatal period [33].

2.3. Experiment 1

Dams were assigned to 5 groups: control, EE 0.02 μg/kg (EE0.02), EE 0.2 μg/kg (EE0.2), EE 20 μg/kg (EE20), and middle-age (6–10 dams/group). The pups of the control and EE groups received a single subcutaneous injection of sesame oil (control) or EE (0.02, 0.2, 20 μg/kg of BW) within 24 h after birth. EE 0.02 μg/kg was selected as the non-inducing and EE 0.2 and 20 μg/kg were selected as the inducing doses of the delayed effect, with reference to a previous report [11]. Litters were culled randomly to preserve 10 pups with a female predominance on postnatal day (PND) 3. On PND 21, the offspring were weaned, and 31–40 female pups per group were housed 3–4 per cage and maintained until 10 weeks of age. Starting on PND 23, we checked the vaginal opening every day. After that, all animals were observed for estrous cycle by vaginal smear for 5 consecutive days every week throughout the experiment. A decision on the cycle pattern was made with every 5-day observation. Regular 4- or 5-day cycles were deemed normal cycles, and other patterns were judged to be abnormal estrous cycles. In particular, animals showing proestrus or estrus continuously for 5 days were designated as having persistent estrus. Observations of clinical signs, body weight, and mortality were made throughout the experimental period. At 10 weeks of age, each rat confirmed as

showing a normal cycle received an OVX under isoflurane anesthesia. One week after OVX, all animals were subcutaneously treated with 2 μg/rat of estradiol benzoate (EB) at 9:00 for 3 consecutive days and 500 μg/rat of progesterone (P4) at 11:00 of the last day of EB treatment for artificial LH surge priming. For the time-course analysis, all animals were decapitated at 11:00 (soon after P4 injection), 14:00, 15:00, 16:00, 17:00 and 19:00 (n = 5–7/time point) of the LH surge priming day and blood samples were collected. The middle-age group was maintained until 22 weeks of age with daily observation of estrous cycle, then divided into 2 groups, one with normal estrous cycle (Middle (N) group, n = 5/time point, total 30 females/group) and another with persistent estrus (Middle (PE) group, n = 4/time point, total 16 females/group). Both groups received the same OVX and LH surge priming treatment and were decapitated at the same times as the control and EE groups, without the time points of 11:00 and 19:00 in the Middle (PE) group. These middle-aged groups were prepared as the animals with spontaneous reproductive aging, and this strain is known to show persistent estrus starting from approximately 4 months of age [8]. Brains were removed from the skulls, and the hypothalami were dissected out as described in a previous report [34] using a horizontal cut about 2 mm in depth with the following 3 limits: 1 mm anterior to the optic chiasm as anterior limit, the posterior end of mammary bodies as posterior limit, and the hypothalamic fissures as lateral limit. Dissected hypothalami were macroscopically divided using the optic chiasm as a boundary into anterior and posterior hypothalamus, which included the AVPV and the ARC,

respectively. The hypothalamic samples were immediately frozen in liquid nitrogen and stored at −80 °C until the time of RNA isolation. The uterus, vagina and mammary glands were also resected from each animal. All organs were fixed in 10% neutral buffered formalin. Tissues were processed routinely and stained with hematoxylin and eosin (HE) for histopathologic examination.

2.4. Hormone assays

Serum samples obtained from decapitation were stored at −80 °C before assay. The serum concentrations of follicle-stimulating hormone (FSH) and LH were determined using double-antibody radioimmunoassays and 125I-labeled radio-ligands. National Digestive and Kidney Disease (NIDDK) radioimmunoassay kits were used for rat FSH and LH with anti-rat LH-S-11 and anti-rat FSH-S-11, as described previously [35]. The intra- and inter-assay coefficients of variations were: 5.09% and 20.75%; 3.45% and 17.40% for FSH and LH, respectively.

2.5. Quantitative real-time PCR

Total RNA was extracted from the hypothalamus lysates using ISOGEN (Nippon Gene Co. Ltd., Tokyo, Japan), and reverse transcription reactions were performed using 1 μg of total RNA with High Capacity Reverse Transcription kits (Applied Biosystems, Foster City, CA, USA). Following the manufacturer's instructions, real-time PCR (7900HT Fast Real-time PCR System, Applied
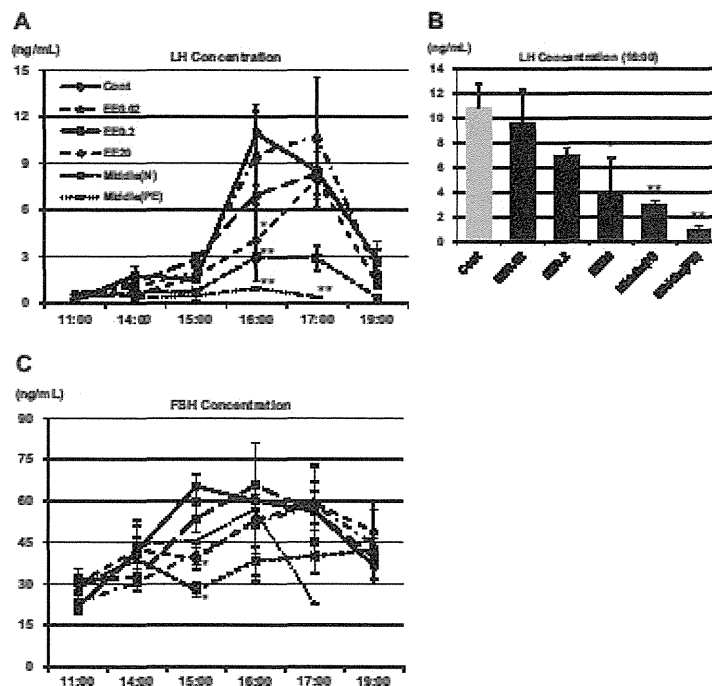

Fig. 1. Sequential changes in serum LH (A) and FSH (C) concentration in EE-exposed and middle-age groups and intergroup comparison of LH concentration at 16:00 (B). EE-exposed groups showed dose-dependent decrease in peak area and concentration of LH at 16:00, and this decrease was more evident in both middle-age groups. Data are presented as mean ± S.E. or mean + S.E. (n = 4–7/group). Symbols indicate significant difference from control group (*p < 0.05 and **p < 0.01 by Dunnett's test, respectively).

Biosystems) was performed using TaqMan® Fast Universal PCR Master Mix (Applied Biosystems) and TaqMan® Gene Expression Assays (Applied Biosystems) as primer–probe sets for the following genes: KISS1 (KiSS1, Rn00710914_m1), KISS1r (KiSS1R, Rn00576940_m1), Esr1 (ERα, Rn01640372_m1), Esr2 (ERβ, Rn00562610_m1) and Fos (c-fos, Rn00487426_g1). The expression level of each gene was calculated by the relative standard curve method and normalized against endogenous GAPDH (TaqMan Rodent GAPDH Control Reagent, Applied Biosystems).

2.6. Experiment 2

For further assessment of kisspeptin neurons, we conducted another experiment to obtain brain samples for in situ hybridization. Dams were assigned to 5 groups (4–9 dams/group). All pups were processed as in Experiment 1 with subcutaneous injection of EE on PND0 for artificial LH surge priming at 11 weeks of age. On the LH surge priming date, all animals were deeply

anesthetized with pentobarbital sodium (Kyoritsu Seiyaku Corporation, Tokyo, Japan) and transcardially perfused with saline followed by 4% paraformaldehyde (PFA, Nacalai Tesque, Inc., Kyoto, Japan) during the interval from 16:00 to 17:00 (n = 4/group). Brains were removed immediately and post-fixed in 4% PFA overnight at 4 °C, then immersed in 30% sucrose/PBS solution at 4 °C until tissues sank. The fixed brains were embedded in O.C.T. compound (Sakura Finetek Japan Co. Ltd., Tokyo, Japan) and blocks were stored at −80 °C until sectioning. The uterus, vagina and pituitary were also resected from each animal. All organs were post-fixed in 4% PFA. Tissues were routinely processed and stained with HE for histopathologic examination.

2.7. In situ hybridization (ISH)

Non-radioactive ISH was used for KiSS1 mRNA-positive cell detection with reference to a previous report [36]. Slides were washed with PBS and treated with 1 μg/mL proteinase K (Takara Bio Inc., Shiga, Japan), followed by brief 1% PFA immersion. After
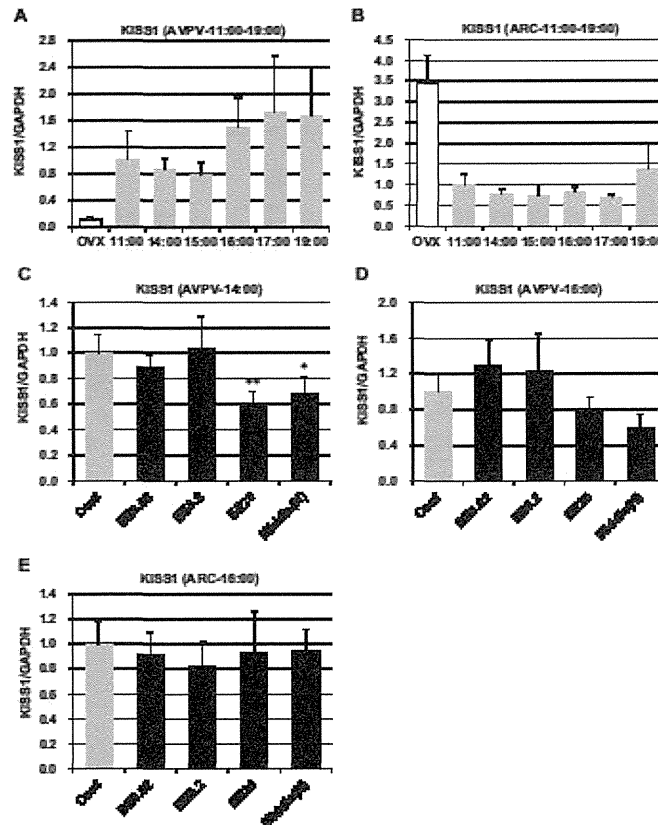

Fig. 2. Sequential changes in KiSS1 mRNA expression in the control group in the AVPV (A) and ARC (B), and intergroup comparison in the AVPV at 14:00 (C) and 16:00 (D) and in the ARC at 16:00 (E). The expression significantly decreased in the EE20 and Middle (N) groups in the AVPV at 14:00, but intergroup differences were not detected in the ARC. All data are presented as mean + S.D. (n = 5/group). Expression level at 11:00 (A and B) or control group (C–E) is adjusted to 1.0. The OVX only group was investigated as a negative control. Symbols indicate significant difference from the control group (*p < 0.05 and **p < 0.01 by Dunnett's test, respectively).

washing in PBS, slides were incubated with 0.25% acetic anhydride in 0.1 M triethanolamine, and then prehybridized with hybridization buffer for 30 min at 60 °C. After prehybridization, slides were hybridized with 0.5 µg/mL of DIG-labeled anti-sense RNA probe (sequence position 3–358, GenBank accession No. AY196983.1, Genostaff, Tokyo, Japan) overnight at 60 °C. A sense RNA probe was used as a negative control. Following hybridization, the slides were washed with 4× SSC/50% formamide, 2× SSC, and 1× SSC. Between SSC washes, slides were briefly immersed in a 20 µg/mL RNase working solution at 37 °C. After washing, slides were blocked with 2% BSA (Sigma, St. Louis, MO, USA) in ISH buffer-1 and incubated with anti–DIG antibody (1:1000, Roche Applied Science, Mannheim, Germany) in ISH buffer-1. Following washing with ISH buffer-1, the slides were immersed in ISH buffer-3 [100 mM Tris–HCl (pH 9.5), 100 mM NaCl, and 50 mM $MgCl_2$] and then incubated with NBT/BCIP solution (Roche Applied Science) in ISH buffer-3 for 1 h.

2.8. Dual-labeling ISH/Immunohistochemistry (IHC)

Following ISH for KiSS1 mRNA, the sections were treated with 1% BSA (Sigma, St. Louis, MO, USA) in PBS and incubated with rabbit anti-ERα (1:2000, sc-542, Santa Cruz Biotechnology Inc., CA, USA) or rabbit anti-c-fos (1:4000, sc-253, Santa Cruz Biotechnology Inc.) overnight. A negative control was incubated without primary antibody. After washing with PBS, the sections were incubated with biotin-conjugated goat anti-rabbit IgG (1:200, Vector Laboratories Inc., CA, USA) in 1% BSA for 30 min. Then the sections were incubated with avidin-biotinylated HRP complex (Vectastain Elite ABC kit, Vector Laboratories Inc.) in PBS for 30 min. The sections were visualized with 3,3-diaminobenzidine-tetrachloride (DAB) mixed with hydrogen peroxide in PBS.

2.9. Sectioning and quantitative analysis of positive cells in ISH and dual-labeling ISH/IHC

In order to evaluate the whole area of the AVPV and ARC, we made sequential coronal sections (20 µm thick) of the AVPV from approximately 0.12 mm anterior to 0.24 mm posterior to the bregma, and of the ARC from approximately 1.72 mm posterior to 3.60 mm posterior to the bregma (Paxinos and Watson, The Rat Brain, 6th edition) using a cryostat (Leica, CM1850UV). After sectioning, all tissue sections were immediately mounted on coated slides (Matsunami Glass Ind., Ltd., Osaka, Japan) and then completely air dried and stored at −80 °C before staining. Since 1 section from every 4 sections from the AVPV and every 15 sections from the ARC was chosen for staining, a total of 4 sections for the AVPV and 6 sections for the ARC per rat were examined. For positive cell counting, an Olympus BX51 microscope with an Olympus digital camera DP73 (Olympus, Tokyo, Japan) was utilized. All KiSS1 mRNA-positive cells with visible reactions in ISH and KiSS1-positive cells with or without ERα/c-fos immunoreactivity in dual-labeling ISH/IHC observed in the lateral half of the brain were manually counted at high magnification in a blinded fashion. The total numbers of KiSS1-positive cells and KiSS1-positive cells with ERα/c-fos immunoreactivity in each group were statistically compared. It was confirmed preliminarily that all sections from the AVPV and ARC had approximately the same number of positive cells in each brain half.

2.10. Statistical analysis

Following Bartlett's test, variances in data for the days of vaginal opening, body and organ weights, hormone assays, real-time PCR and numbers and percentages of ISH or dual-labeling ISH/IHC positive cells were compared with those for the control group by
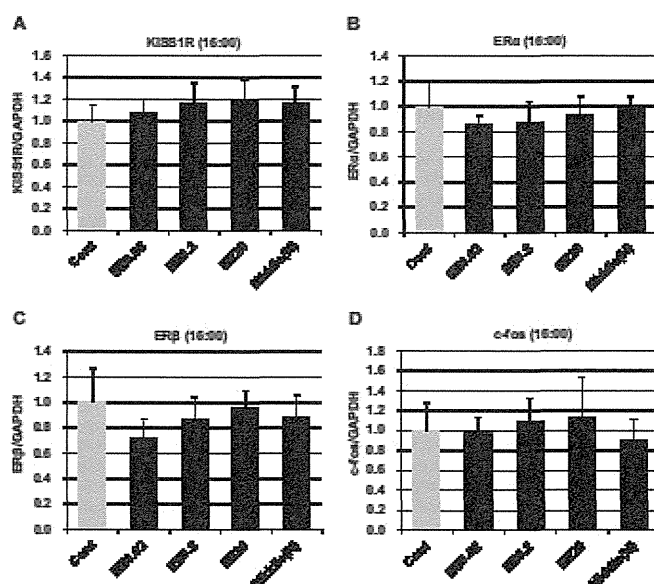

Fig. 3. mRNA expression of KiSS1R (A), ERα (B), ERβ (C), and c-fos (D) in the AVPV at 16:00. No intergroup difference was detected for any KiSS1-related gene. All data are presented as mean + S.D. (n = 5/group). Expression level of the control group is adjusted to 1.0.
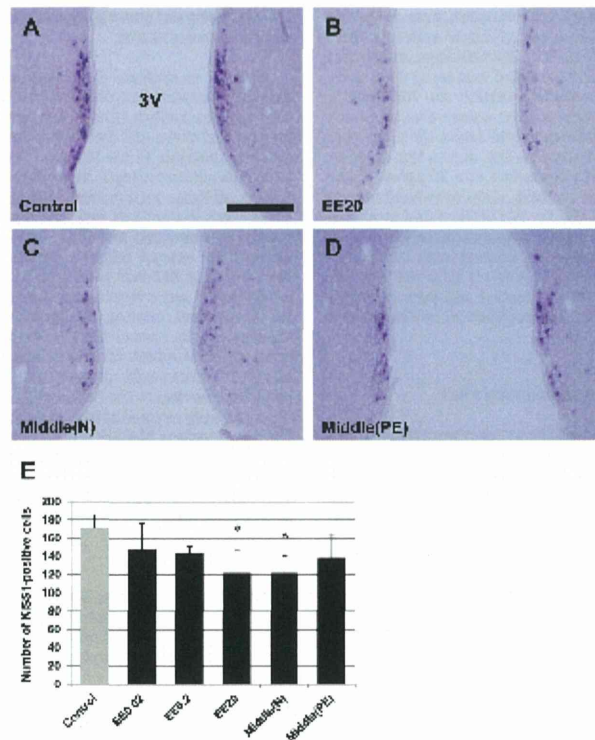
Fig. 4. Representative images of KISS1 mRNA-positive cells in the AVPV in control (A), EE20 (B), Middle (N) (C) and Middle (PE) (D) groups. The number of positive cells was significantly decreased in the EE20 and Middle (N) groups (E). All brain samples were collected during the interval from 16:00–17:00. All data are presented as mean + S.D. (n = 4/group). Symbols indicate significant difference from the control group (*p < 0.05 by Dunnett's test). 3V: third ventricle. Scale bar = 200 μm.

one-way analysis of variance or the Kruskal–Wallis test. When statistically significant differences were detected, Dunnett's multiple comparison test was employed for comparisons among the control group, EE-exposed groups and middle-age groups. In these tests, the level of significance was set at 0.05.

3. Results

3.1. Clinical observation, estrous cycle, and ovarian histology

No abnormalities or deaths were observed throughout the experimental periods. Significant increases in body weight were observed in all EE groups during weeks 4 and 5; however, these changes were transient, and no intergroup differences were observed after week 6 (data not shown). No significant differences were detected in the mean days of vaginal opening between each group (data not shown). All animals, except those in the Middle (PE) group, were confirmed to have normal estrous cycles before OVX by daily observation of vaginal smears. After OVX, vaginal smear showed a pattern similar to that of diestrus in all animals, and cornified smears were observed after EB treatment for 3 days. Estrous cycles determined by ovarian histology coincided well with those determined by vaginal smears, and no histological difference at each cycle was found between the control group and EE-exposed

groups. In middle-age groups, several animals in the Middle (N) group showed a decreased number of recent corpora lutea, which may indicate a possibility of occurrence of anovulation status in resent several cycles, although the vaginal smears indicated normal estrous cycles. Most animals in the Middle (PE) group showed a lack of recent corpora lutea and cystic atresia, which reflects prolonging anovulation status in this group.

3.2. Serum concentration of LH and FSH

Sequential changes in serum LH concentrations are shown in Fig. 1. LH concentrations were markedly increased during the interval from 16:00 to 17:00 in the control and EE-exposed groups, but the peak time of LH concentrations were delayed in EE-exposed groups as it detected at 16:00 in the control group and 17:00 in the EE-exposed groups. In the middle-age groups, a slight increase in LH concentrations at 16:00–17:00 was observed in the Middle (N) group, and the Middle (PE) group was almost near the baseline throughout the measurement period. In addition, the peak areas of the LH surges in the EE-exposed and middle-age groups clearly decreased compared to that of the control group. On the other hand, the peak area in the EE0.02 group was almost the same as that detected in the control group (Fig. 1A). In intergroup comparisons at each time point, the serum LH concentrations were significantly

decreased in the EE20, Middle (N) and Middle (PE) groups at 16:00, and a slight decrease was observed in the EE0.2 group (Fig. 1B). Sporadic increases or decreases were also observed at other time points; however, these changes were considered to be incidental due to lack of consistency and dose dependency. Serum FSH concentrations were moderately increased beginning in the afternoon, peaking at 15:00 in the control group and 16:00–17:00 in the EE-exposed groups. A significant decrease was observed in the EE0.02 and EE20 groups at 15:00. The FSH concentration of the Middle (N) group was not increased throughout the measurement period and significantly decreased from the control group at 15:00 (Fig. 1C).

3.3. Quantitative real-time PCR

Sequential changes in KiSS1 mRNA expression in the AVPV and ARC of the control group and intergroup comparisons are shown in Fig. 2. In the AVPV, obvious expression of KiSS1 mRNA was detected from 11:00 and peak expression was observed during the interval from 16:00 to 17:00, the same as the peak time of LH surge in the present study. This peak expression continued to be detected at 19:00 (Fig. 2A). In the ARC, expression of KiSS1 mRNA was suppressed throughout the measured time points when compared to expression in the OVX-only group, and expression slightly recovered at 19:00 (Fig. 2B). Intergroup comparison revealed that KiSS1 mRNA expression in the AVPV of the EE20 and Middle (N) groups was significantly decreased at 14:00, and this decreasing trend continued to be observed in both groups at 16:00, although the decrease was not statistically significant at this time point (Fig. 2C and D). On the other hand, no intergroup differences were detected in KiSS1 mRNA expression in the ARC at 16:00 (Fig. 2E). The mRNA expression of KiSS1-related genes is shown in Fig. 3. Although a clear decrease in KiSS1 mRNA expression in the AVPV was detected in the EE20 and Middle (N) groups, expression of KiSS1R, ERα, and ERβ mRNA was not significantly changed among the control, EE-exposed, or Middle (N) groups (Fig. 3A–C). In addition, c-fos expression, which was examined as a marker of neuronal activity in the kisspeptin neurons, was also not changed among the experimental groups (Fig. 3D).

3.4. In situ hybridization

Representative KiSS1 mRNA-positive cells in the AVPV and ARC are shown in Figs. 4 and 5, respectively. In the AVPV, most KiSS1-positive cells were located around the third ventricle (3V), and the
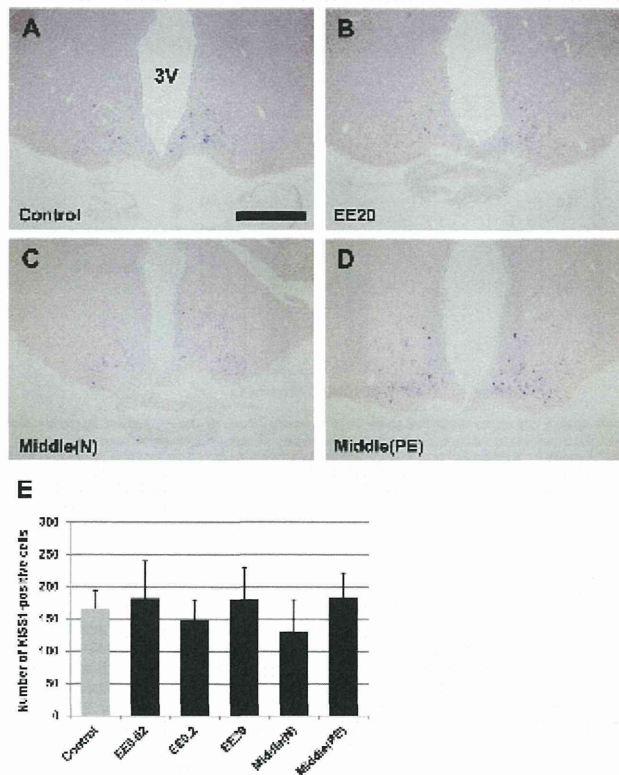

Fig. 5. Representative images of KiSS1 mRNA-positive cells in the ARC in control (A), EE20 (B), Middle (N) (C) and Middle (PE) (D) groups. No intergroup differences in the number of KiSS1-positive cells were detected in the ARC (E). All brain samples were collected during the interval from 16:00 to 17:00. All data are presented as mean + S.D. (n = 4/group). 3V: third ventricle. Scale bar = 500 μm.
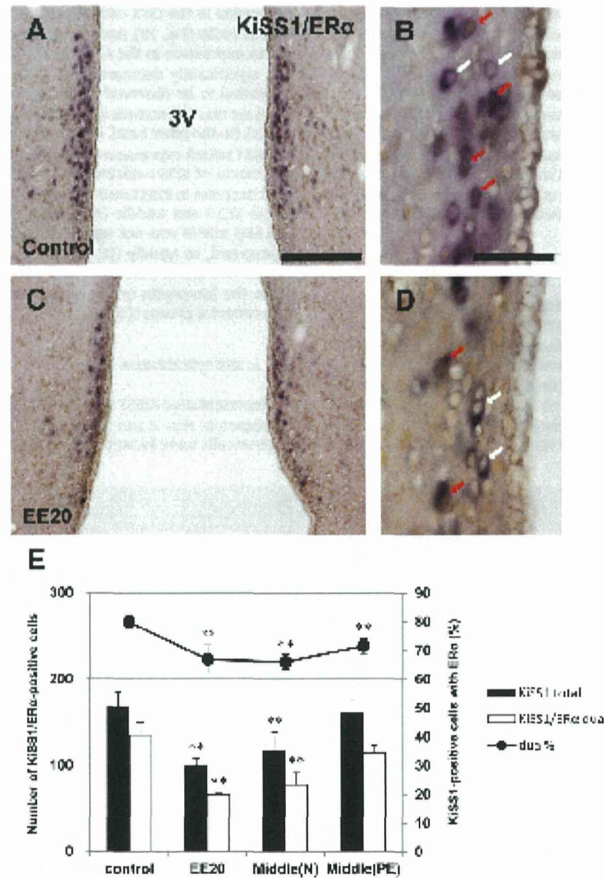
Fig. 6. Representative images of dual-labeling ISH/IHC for KiSS1/ERα in the AVPV in control (A and B) and EE20 (C and D) groups. Most positive cells show dark blue cytoplasmic staining for KiSS1 mRNA and brown nuclear staining for ERα. Red arrows represent KiSS1/ERα-double positive cells and white arrows represent KiSS1 mRNA-single positive cells. Percentage of KiSS1-positive cells showing nuclear ERα immunoreactivity significantly decreased in EE20, Middle (N) and Middle (PE) groups (E). Graph shows the total number of KiSS1-positive cells (closed bar), the number of KiSS1/ERα double positive cells (open bar) and percentage of KiSS1-positive cells showing ERα co-expression (line chart). All brain samples were collected during the interval from 16:00 to 17:00. Data are presented as mean ± S.D. or mean + S.D. (n = 4/group). Symbols indicate significant difference from the control group (**: p < 0.01 by Dunnett's test). 3 V: third ventricle. Scale bars = 200 μm (A and C) or 50 μm (B and D).

number of KiSS1 mRNA-positive cells (half brain) was significantly decreased in the EE20 and Middle (N) groups and slightly decreased in other EE-exposed groups (Fig. 4E). In addition to decrease in the number of positive cells, attenuation of KiSS1 mRNA signals in each positive cell was observed in the EE20 and Middle (N) groups relative to that in the control group (Fig. 4A–C). Interestingly, on the other hand, KiSS1 mRNA intensity in each positive cell seemed to be slightly recovered in the Middle (PE) group (Fig. 4D). In the ARC, KiSS1 mRNA-positive cells were located in the lower periventricular area of the 3V. In contrast to the AVPV, the number and intensity of KiSS1-positive cells in the ARC were not significantly changed among the control, EE-exposed, or middle-age groups (Fig. 5A–E).

3.5. Dual-labeling ISH/IHC

Representative KiSS1 mRNA-positive cells with ERα/c-fos immunoreactivity are shown in Figs. 6 and 7, respectively. In dual-labeling staining with KiSS1 and ERα/c-fos, dual positive cells showed dark blue cytoplasmic staining for KiSS1 mRNA and brown nuclear staining for ERα/c-fos (red arrows), and KiSS1-single positive cells only showed cytoplasmic staining for KiSS1 (white arrows) (Figs. 6A–D and 7A–D). In dual staining with KiSS1 and ERα, most KiSS1-positive cells showed positive nuclear immunoreactivity for ERα and the percentage of KiSS1-positive cells co-expressing ERα reached 79.9% in the control group. Compared to the control group, the number of KiSS1/ERα-dual
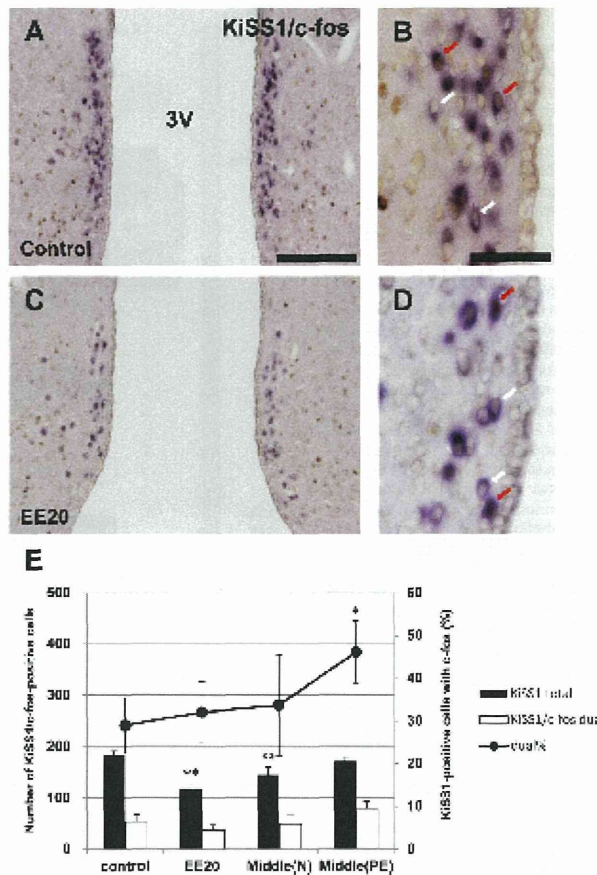
Fig. 7. Representative images of dual-labeling ISH/IHC for KiSS1/c-fos in the AVPV in control (A and B) and EE20 (C and D) groups. Most positive cells show dark blue cytoplasmic staining for KiSS1 mRNA and brown nuclear staining for c-fos. Red arrows represent KiSS1/c-fos-double positive cells and white arrows represent KiSS1 mRNA-single positive cells. Percentage of KiSS1-positive cells showing nuclear c-fos immunoreactivity was not changed in EE20 and Middle (N) groups, but significantly increased in Middle (PE) group (E). Graph shows the total number of KiSS1-positive cells (closed bar), the number of KiSS1/c-fos double positive cells (open bar) and percentage of KiSS1-positive cells showing c-fos co-expression (line chart). All brain samples were collected during the interval from 16:00 to 17:00. Data are presented as mean ± S.D. or mean + S.D. (n = 4/group). Symbols indicate significant difference from the control group (*: $p < 0.05$ and **: $p < 0.01$ by Dunnett's test, respectively). 3 V: third ventricle. Scale bars= 200 μm (A and C) or 50 μm (B and D).

positive cells was significantly decreased in EE20 and Middle (N) groups, and the percentage of KiSS1-positive cells with ERα expression was also significantly decreased to 66.8% and 66.1% in EE20 and Middle (N) groups, respectively (Fig. 6E). In dual staining with KiSS1 and c-fos, the number of KiSS1/c-fos-dual positive cells was not significantly changed in these groups, and the percentage of KiSS1-positive cells co-expressing c-fos were 28.9%, 32.0% and 33.7% in control, EE20 and middle (N) group, respectively. In contrast, the number of KiSS1/c-fos-dual positive cells in Middle (PE) group slightly increased, and the percentage of KiSS1-positive cells with c-fos expression was reached 46.1%, significantly increased compared to that of control group (Fig. 7E).

4. Discussion

Kisspeptin is one of the most recently discovered neuropeptides and is a central regulator of GnRH and gonadotropin secretion in the HPG axis, consequently controlling various reproductive functions, including estrous cycle, ovulation, and follicular development [17,18]. Kisspeptin plays a site-specific role in regulating ovulation by induction of preovulatory LH surges through positive feedback in the AVPV [24] and regulating folliculogenesis through pulsatile GnRH secretion in the ARC. In previous studies, we reported the early onset of age-related abnormal estrous cycles in neonatally EE-exposed rats [11], indicating some sort of disruption in neuroendocrine pathway. Thus, we investigated the changes in the LH

surge and KiSS1 mRNA expression in normally cycling young adult animals neonatally exposed to EE.

In the present study, real-time PCR analysis revealed that KiSS1 mRNA expression in the AVPV peaked at 16:00–17:00, the same time as the peak of LH surge in each group. This result indicates rapid transmission of kisspeptin and GnRH neuron, which results in quick gonadotropin secretion from the pituitary. In intergroup comparisons, KiSS1 mRNA expression in the AVPV at 14:00 was significantly decreased in the EE20 and Middle (N) groups, to nearly half the level of the control group, and the decreasing trend was maintained up to 16:00 in both groups. Furthermore, in the more site-specific analysis by ISH, we found that the number of KiSS1 mRNA-positive cells and their signal intensities in the AVPV were significantly decreased in the EE20 and Middle (N) groups. These results clearly indicate the down-regulation of KiSS1/GPR54 signaling and neurotransmission in the HPG axis at the time of the LH surge, suggesting the attenuation of the reactivity to exogenous estrogenic treatment in delayed effect and middle-aged animals. In addition, we also found that the number and percentage of KiSS1/ERα-dual positive cells were significantly decreased in these groups, possibly indicating that down-regulation of KiSS1 signaling might be related to the decrease of ERα expression. These results also mean that a single treatment with EE at PND 0 induces attenuation of KiSS1 mRNA expression in the AVPV even approximately 2 months earlier than the occurrence of early onset of abnormal estrous cycling reported in our previous study [11]. On the other hand, in the ARC, no statistically significant change was observed in KiSS1 mRNA expression at 16:00, and the number and intensity of KiSS1-positive cells were also not changed among control, EE-exposed, and middle-age groups. Therefore, it could be said that the attenuation of KiSS1 mRNA expression in the delayed effect and middle-aged rats was specific to the AVPV, and, thus, follicular development may not be influenced by the delayed effect.

Regarding other KiSS1-related genes, none of the investigated genes (KiSS1R, ERα, ERβ and c-fos) exhibited any significant differences in mRNA expression detected by quantitative real-time PCR. The discrepancy of ERα expression between real-time PCR and dual-labeling ISH/IHC might be due to abundant ERα expressing cells other than the kisspeptin neuron in the area surrounding 3V, thus the site-specific assay like a dual-labeling ISH/IHC is considered to be more robust technique for detection of common molecules in the kisspeptin neuron. In contrast, consistent with the results in real-time PCR, percentage of KiSS1-positive neuron with c-fos immunoreactivity was not changed in EE20 and Middle (N) groups. In previous studies, c-fos co-expression in kisspeptin neurons was clearly related to the functional activity of kisspeptin neurons and the following LH surge [20,23]. Recently, Ishii et al. [36] also reported that the percentage of KiSS1 mRNA-positive cells with c-fos immunoreactivity decreased in middle aged female rats. In these studies, percentage of c-fos co-expression in activated kisspeptin neuron reached nearly 60%. The precise reason is not determined, but the lower percentage of c-fos co-expression in our control group might contribute to this contradictory result. On the other hand, the percentage of KiSS1/c-fos-dual positive cells in Middle (PE) group significantly increased in our study, indicating the increased reactivity to estrogens in this group. This may result from the possible imbalance of feedback system in this acyclic group associated with the cessation of estrous cycle, but this hypothesis needs to be verified by further investigation.

Assay of serum LH concentrations in the control group indicated that the peak time of LH surge in the environment of our facility was at 16:00, although those of all EE-exposed groups were at 17:00. In addition, dose-related reduction of the LH peak area and peak concentration at 16:00 was observed in the EE20 and EE0.2 groups, and these decreases were more evident in the Middle (N) and (PE) groups, indicating reduced peak amplitude and delayed peak time
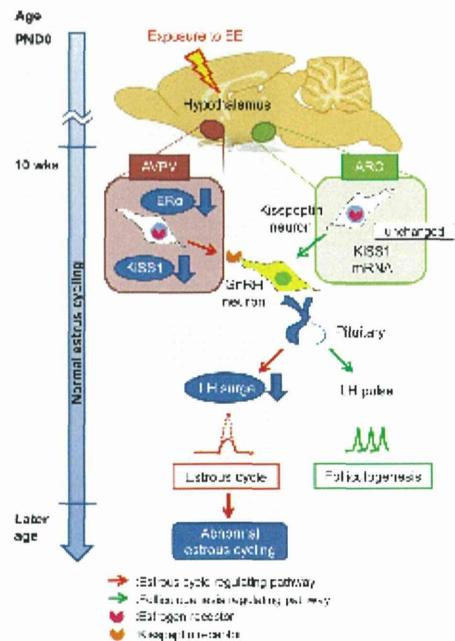

Fig. 8. Proposed pathway for the delayed effect. Neonatal exposure to EE induces an AVPV-specific decrease in KiSS1 and ERα mRNA expression and a consequent attenuation of LH surge in young adult rats, leading to the early onset of abnormal estrous cycling.

for the LH surge. Since activation of hypothalamic kisspeptin and GnRH neurons is essential for the induction of the preovulatory LH surge [23], it is highly possible that the depression in KiSS1 mRNA expression observed in the present study leads to these functional changes in the LH surge. The attenuation of LH surge could also contribute to the cessation of ovulation and early onset of abnormal estrous cycling in the delayed effect. The proposed pathway is shown in Fig. 8.

Attenuation and delay of the LH surge are normal senescence processes of the estrous cycle in middle-aged rats [37–39], and these changes associated with aging have also been reported to precede the cessation of regular estrous cycling [40]. Recently, moreover, not only the alteration in the LH surge, but also attenuation of KiSS1/GPR54 signaling in the hypothalamus of middle-aged rats have been reported in several articles [28,29,41], suggesting depression of kisspeptin neuron might be a trigger for age-related LH surge dysfunction and reproductive aging [28]. In the present study, we confirmed the similar serial dysfunction of the kisspeptin neuron and LH surge in young adult animals neonatally exposed to EE. Similar to reproductive aging and the delayed effect, high dose neonatal exposure to various estrogenic compounds such as bisphenol-A, 17alpha-ethynylestradiol, estradiol benzoate, and selective ERα agonists also showed attenuation of the LH surge [42,43], KiSS1 mRNA expression, and/or immunoreactivity for kisspeptin in the hypothalamic kisspeptin neurons [30–32].

Another important finding in the present study is the fact that all these hypothalamic and hormonal changes occurred before the onset of abnormal estrous cycling, indicating that the disruption